

8. PHOTODETECTORS

The Hadron Calorimeter is composed of several subsystems. HB and HE are situated directly in the 4 T solenoid field, and to keep the detected light yields at a reasonable level, the phototransducers must be located within the field volume. The Outer Calorimeter systems, HBO and HOE, are located within the barrel and endcap muon systems, and photosensors can be placed at the outer perimeter of the CMS muon yokes and rings. Hence residual and leakage fields from the muon steel can be screened out for these photosensors by careful attention to magnetic shielding. The HF subsystems are located forward and backward along the beam, beyond the endcap muon detectors. Here radiation damage is the principal concern, and magnetic shielding is a minor issue.

These issues, plus the substantial channel counts per subsystem, and the need to maintain a reasonable per channel cost, impose the requirement of commonality (where possible) among system elements - particularly the phototransducers and associated front-end electronics. In the long term, the fewer distinct systems to maintain the better. For HB and HE, the photodetector is the Hybrid Photodiode (HPD), a proximity-focused photomultiplier tube with a silicon target, which can operate effectively in high magnetic field. Because the HPD is a pixel device (19-, 25-, 61-, and 73-channel HPDs are under consideration), the cost per channel can be reduced substantially. For HBO and HOE, the magnetic field issues do not apply, but the channel count for these systems is large. Commonality with HB and HE systems dictates that the appropriate photosensor for these subsystems is also the HPD. For HF, where quartz calorimetry is utilised to provide excellent physics (shower) measurement in the presence of a significant radiation field, higher gain is required. Here conventional photomultiplier tubes with quartz or boron-free glass windows are the preferred solution.

8.1 HADRON CALORIMETER PHOTODETECTORS

8.1.1 HB/HE requirements

There are several important requirements imposed on the photosensor used in the inner barrel (HB) and inner endcap (HE) calorimetry.

Magnet Field: The HB/HE photodetectors must operate in a 4 tesla field.

Linearity of Response: The transducer must be linear over a range of signals from minimum ionising to 3 TeV hadron showers. The need to detect muons via their small, minimum-ionising signal, specifies an excellent signal to noise ratio.

Leakage/Dark Current: The scintillator towers must be calibrated to 1% using a radioactive source mounted on a remote-controlled retractable wire.

Lifetime: The photodetector must operate adequately for at least 10 years of LHC operation, which corresponds to an integrated output charge of ~ 3 Coulombs and to an integrated neutron dose of $\sim 5 \times 10^{10}$ n/cm².

Results from studies performed both in laboratory bench tests and at the CERN test beam have shown that HPDs meet the above criteria.

The HPD consists of a photocathode followed by a gap of several millimetres over which a large applied electric field accelerates the photoelectrons onto a silicon target. (See Fig. 8.1) The gain of such a device is therefore given by the acquired kinetic energy of the photoelectrons (above some threshold energy which depends on the surface treatment of the diode) divided by

the 3.6 eV required to release an electron-hole pair in the diode. For an applied voltage of 15 kV, a gain of approximately 3000 is realised. The response curve and extracted absolute gain curve are shown in Fig. 8.2 for a commercially available 7 channel HPD from DEP[1]. The photocathode is S20 with a fibre optic window and effective quantum efficiency of 12% in the green ($\lambda \sim 500$ nm). The ability to measure to 1% a small DC current above background fluctuations imposes an additional requirement on the transducer.

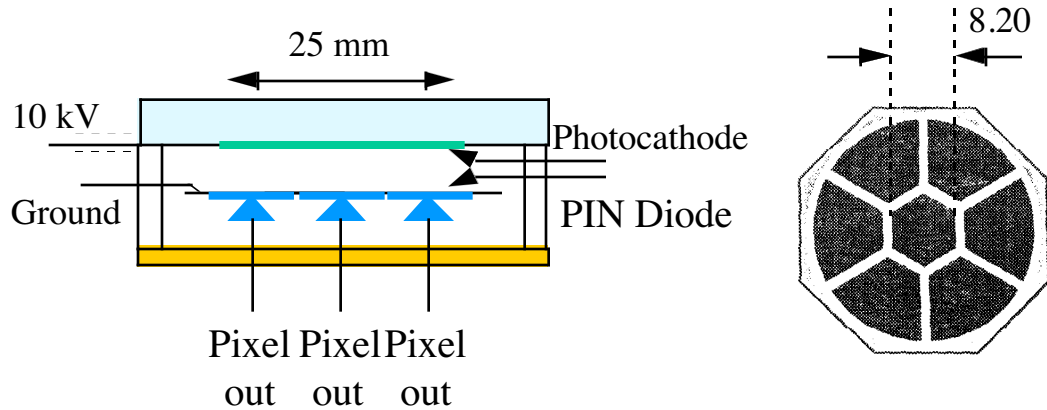


Fig. 8.1: HPD Schematic and tube structure.

Fig. 8.2: Response and absolute gain for a 7-channel HPD.

8.1.2 HOB and HOE photodetector requirements

The Outer Calorimeter systems HOB and HOE are expected to supply approximately 10 p.e./m.i.p. if a PMT were used. Since the function of the HO detectors is to tag muons and to tag and measure late developing showers, there are not very stringent requirements on the photo-transducer. Indeed, since the HPD has sufficient performance to meet these requirements, and since the commonality argument is compelling, we also chose HPDs for the HO detectors as the baseline.

8.2 HPD measured Characteristics

Several characteristics of DEP HPDs were measured on the bench. Transducers with 1, 7 and 25 pixels were used. The photocathode uniformity was measured by scanning a light beam across the 7 pixel device. The uniformity observed was excellent, as shown in Fig. 8.3. The Si layer of the 25 pixel device is shown in Fig. 8.4. The gain uniformity as a function of high

8. PHOTODETECTORS

voltage and at fixed high voltage for all 25 pixels is shown in Fig. 8.5 and Fig. 8.6. Clearly, the linearity and gain uniformity requirements are met by the DEP device.

The resolution of response to a fixed amount of light (7 pixel device) is shown in Fig. 8.7. Clearly, no long tails are observed and the response is very well represented as a Gaussian over 4 orders of magnitude. The resolution of the 7 pixel device at fixed incident light intensity and PIN diode bias, but variable high voltage is shown in Fig. 8.8. At very large voltages a high level tail appears. We ascribe it to secondary charge liberated from the residual gas in the tube. These and other observations caused us to place a strict requirement on residual gas in the device.

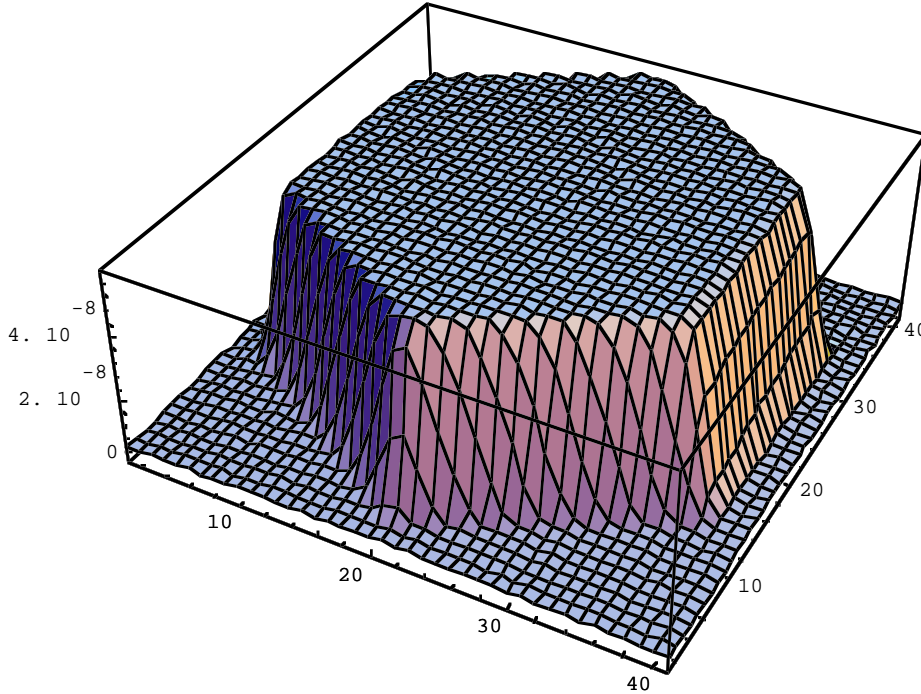


Fig. 8.3: The result of a scan of the central pixel . This plot shows current in nA for the central pixel $\times 10^{-1}$ versus position on the face of the HPD (in 250 nm increments).

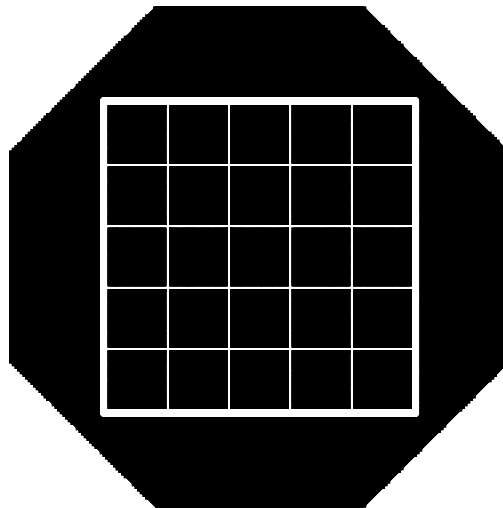


Fig. 8.4: Layout of the 25 pixel device.

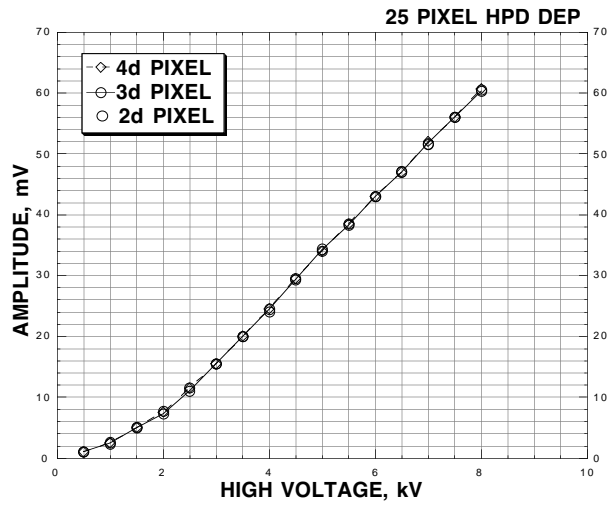


Fig. 8.5: Pixel to pixel response of gain vs. high voltage.

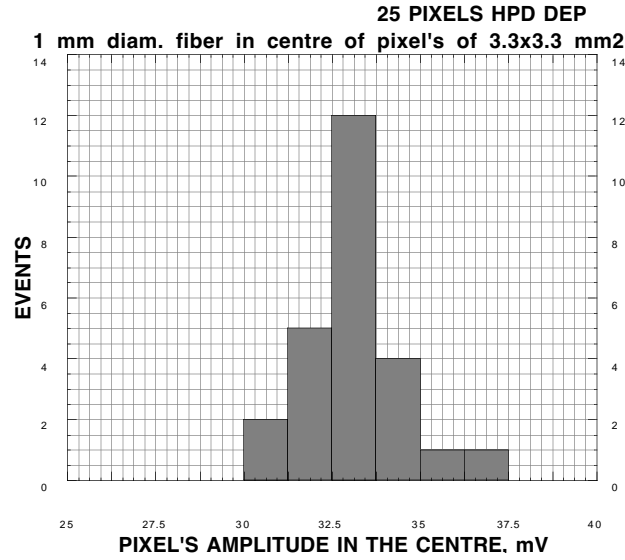


Fig. 8.6: Mean gain for each pixel (25 pixel HPD) at fixed high voltage.

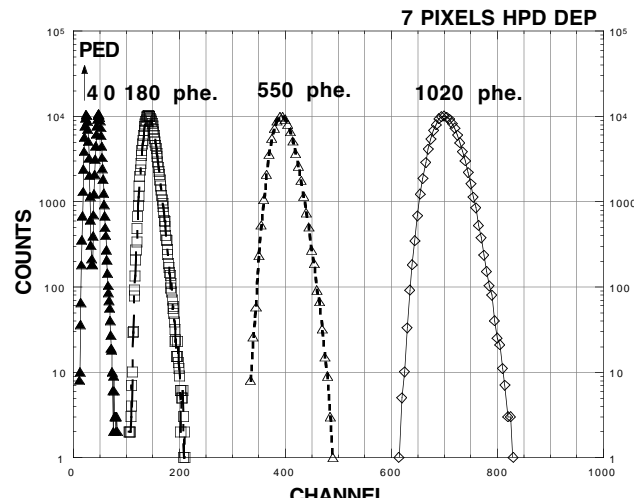


Fig. 8.7: Pulse response of 7 pixel device to different light levels at fixed high voltage



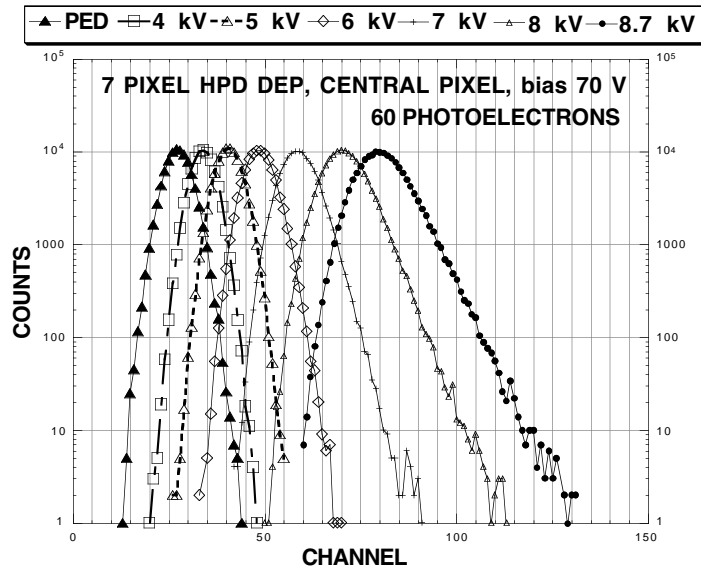


Fig. 8.8: Pulse response of the 7 pixel device at fixed light level and fixed diode bias as a function of high voltage

We have also studied the pulse shape of the device. For technical reasons the diode is backside illuminated, which means that we collect holes at the grounded anode of the PIN diode. The physics event rates involved require d.c. coupling. Hence we have a rise time set by the hole drift across the 300 μ m depth of the diode, since the bombarding 10kV electrons have only about a 15 μ m range in silicon. The observed rise and fall times of a 25 pixel device (minimum source capacity) are shown in Fig. 8.9 as a function of diode voltage. Full depletion occurs at approximately 70V, so that the device must be run heavily overdepleted to achieve a rise time which is less than the 25ns bunch spacing.

Since the scintillator tile + WLS fibre time constant is about 12 ns, it is unacceptable to have such a slow device with an intrinsically fast technology. The diode can be thinned to 150 μ m, which halves the rise time. We are negotiating with DEP to have thinned prototype devices as soon as possible.

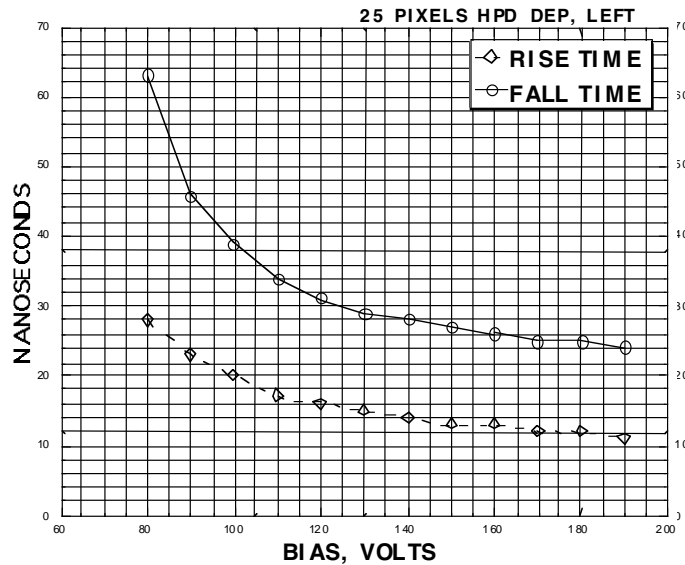


Fig. 8.9: Rise and fall times as a function of the diode bias.

8.3 HPD CHARACTERISTICS FROM TEST BEAM AND RADIATION EXPOSURE

8.3.1 Response to particles - muons

A prototype HB stack was read out by both APDs and HPDs in several beam tests at CERN in 1995 and 1996. Electron and hadron energy resolutions were the same as measured with standard phototubes, and were determined only by the sampling fluctuations of the shower and the calorimeter design. On the other hand, the low-light performance was found to be distinctive dependent upon the choice of phototransducer. A high energy muon (m.i.p.) recorded in 10 layers of scintillator produced a mean signal of 7.5 p.e. for a standard PMT, 6.5 p.e. for a HPD, and 45 p.e. for a silicon APD (as confirmed by LED studies). However, this mean signal was detected with a signal-to-noise ratio (defined as the mean of the signal divided by the pedestal width) of 59 for the PMT, ~ 8 for the HPD and ~ 2.4 for the best APD channel. The muon results are shown in Fig. 8.10. Note that the data confirm the observation that HPDs meet the requirement of clean muon detection for the HO transducers.

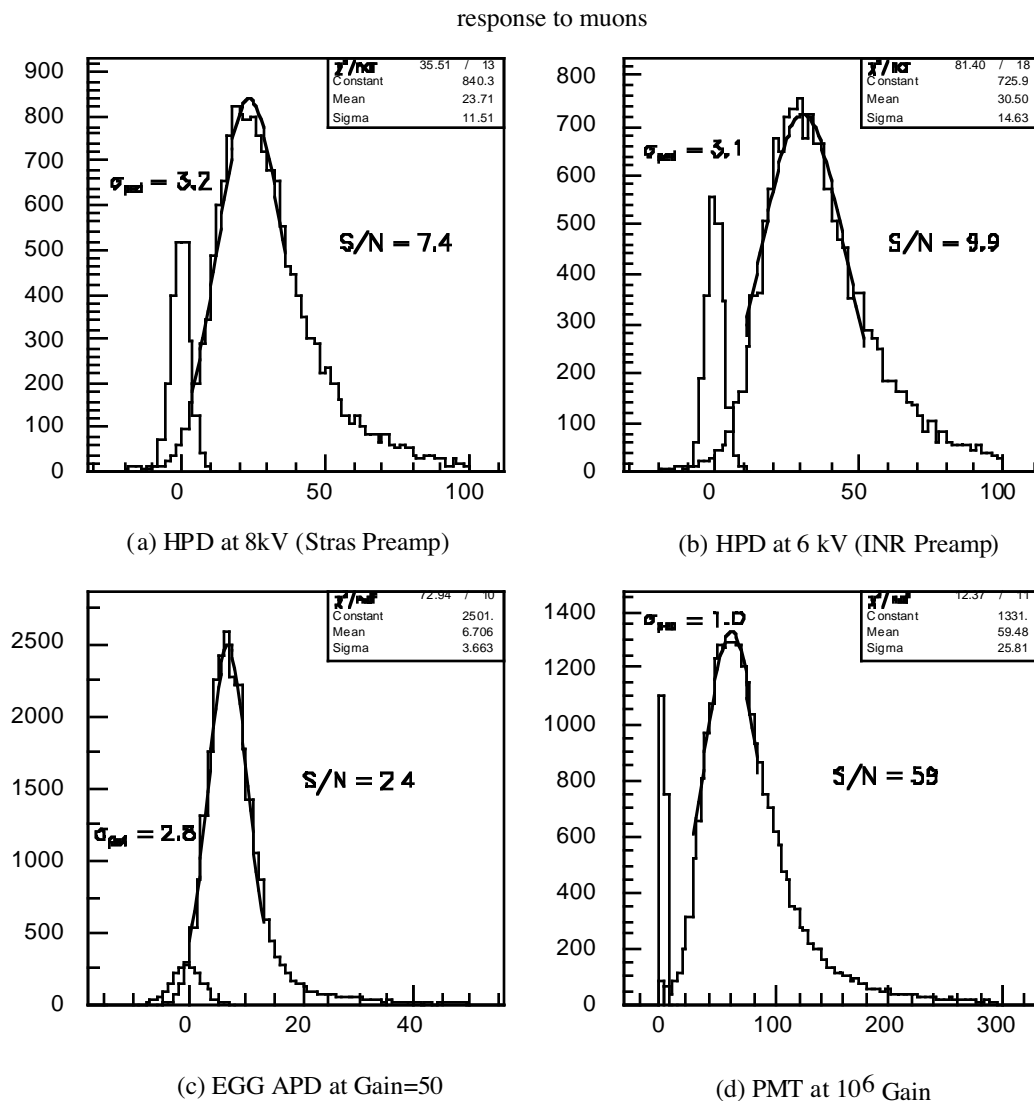


Fig. 8.10: Photodetector comparison for minimum ionising particles: ADC signal and pedestal for muons.

8. PHOTODETECTORS

8.3.2 DC response and calibration to Cs source

Source current measurements were also made at the test beam. As the 5 mC source passed across each tile in the calorimeter stack, custom 7-channel op-amp conditioning circuits mounted directly on the electronics box in the beamline converted the HPD current to a voltage which was read out by a peak-sensitive scanning ADC. Trim pots on each channel zeroed out the leakage current (5-10 nA) which was of the same order as the expected DC signal. Since it is the fluctuation on the background current rather than its level that determines the signal-to-noise, the ratio $\text{rms}/I_{\text{source}}(\%)$ gives the percent sensitivity that can be achieved. A comparison of PMT and HPD results for the same two towers (first 4-layers) is compiled in Table 8. 1. On average, one can make current measurements to 0.7% with the HPD and none are larger than the 1% specification.

Table 8. 1

Comparison between HPD and conventional PMT during radioactive source calibration at the 1995 CERN test beam. Source current (I_{source}), dark current (I_{bkgd}), and fluctuations in dark current (rms) measured in nanoamps.

Layer	Tower 5		HPD		Tower 6		PMT		Tower 6	
	$I_{\text{bkgd}} - \text{rms} =$		$I_{\text{bkgd}} - \text{rms} =$		$I_{\text{bkgd}} - \text{rms} =$		$I_{\text{bkgd}} - \text{rms} =$		$I_{\text{bkgd}} - \text{rms} =$	
	-0.3192 - 0.0369		-0.1753 - -0.0316		3.095 - 0.1719				2.992 - 0.1814	
	I_{sfc}	$\text{rms}/I_{\text{sfc}}(\%)$	I_{sfc}	$\text{rms}/I_{\text{sfc}}(\%)$	I_{sfc}	$\text{rms}/I_{\text{sfc}}$	I_{sfc}	$\text{rms}/I_{\text{sfc}}(\%)$	I_{sfc}	$\text{rms}/I_{\text{sfc}}(\%)$
1	4.9	0.753	5.3	0.596	-	-	-	-	-	-
2	5.8	0.636	4.7	0.672	314.	0.055	251.	0.072		
3	4.3	0.858	5.8	0.545	294.	0.058	298.	0.061		
4	5.8	0.636	4.8	0.658	342.	0.050	249.	0.073		

8.3.3 Lifetime and radiation damage

The photodetector lifetime is affected by both the intensity of the signal itself and by radiation damage. The maximum integrated charge collected at the output (assuming an operating gain of 3000) is expected for an HE tower which samples shower maximum at highest jet energies ($|\eta| = 3$) and is 15 Coulombs over 10 years. Two HPDs have been operated under monitored illumination at DEP for 6 months and their gain as a function of time is shown in Fig. 8.11. Tube E18 is an electrostatically focused tube (with a getter) operated at 15 kV and Tube P25 is a 7-channel proximity focused tube (without getter) operated at 11 kV. The reverse diode bias in both cases is at 25V. At present, no change in gain has been recorded after 0.44 C of integrated charge in the tube with the getter. The tube without getter has a 30% loss in signal. A getter is therefore required for the CMS tube. We will continue to observe these tubes for another year in order to insure that at least 15Coulombs can be pulled off the anode.

The maximum integrated radiation dose of neutrons is expected to be 5×10^{10} n/cm² for photodetector boxes of HB/HE. To measure the effects of integrated dose, a 7-channel DEP tube was irradiated by moderated (1 MeV) neutrons from seven distributed ²⁵²Cf sources at Oak Ridge National Laboratory with a total fluence of $(3.5 - 0.3) \times 10^{10}$ n/cm²/hour at the surface of the photodetector. The HPD was operated at high voltage and bias during the irradiation, and both a centre and side pixel were monitored by blue light piped through rad-hard fused silica optical fibres. As can be seen from Fig. 8.12, both pixels reacted to neutron irradiation with a monotonically increasing leakage current typical of silicon. When normalised to the area of the pixel (58 and 72 mm² for central and side pixel respectively), this corresponds to a rate of

increase of $20 \text{ nA} / 10^{10} \text{ n} / \text{cm}^2$. For CMS HPDs with pixel areas of 6.25 and 25 mm^2 , the leakage current would rise to 6 and 24 nA after an integrated dosage of $5 \times 10^{10} \text{ n/cm}^2$. When exposed to doses an order of magnitude larger than expected (as high as 10^{13} n/cm^2), the HPDs continued to operate properly, although photocathode damage resulted in a 30% reduction in the signal and leakage currents rose to mA . The rms fluctuations in the leakage current, however, were still measured to be 16 pA , meaning that a 1% DC source current calibration should still be possible.

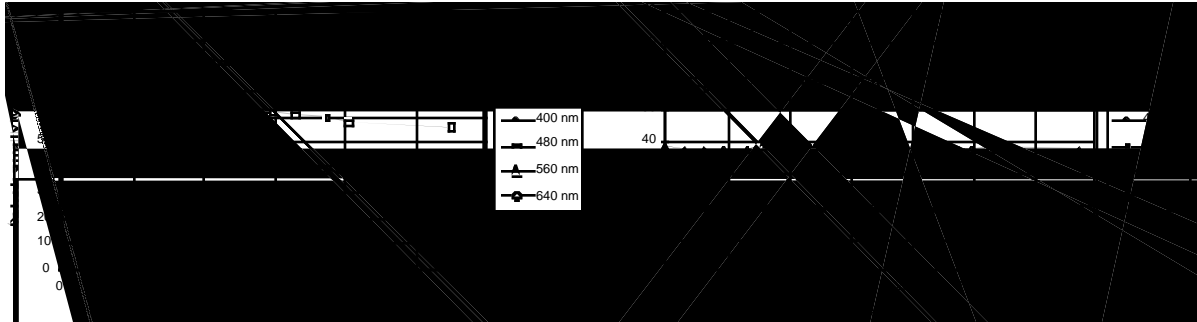


Fig. 8.11: Lifetime of DEP HPD under constant illumination: Gain vs. integrated charge at output. Left side is P25 and right side is E18.

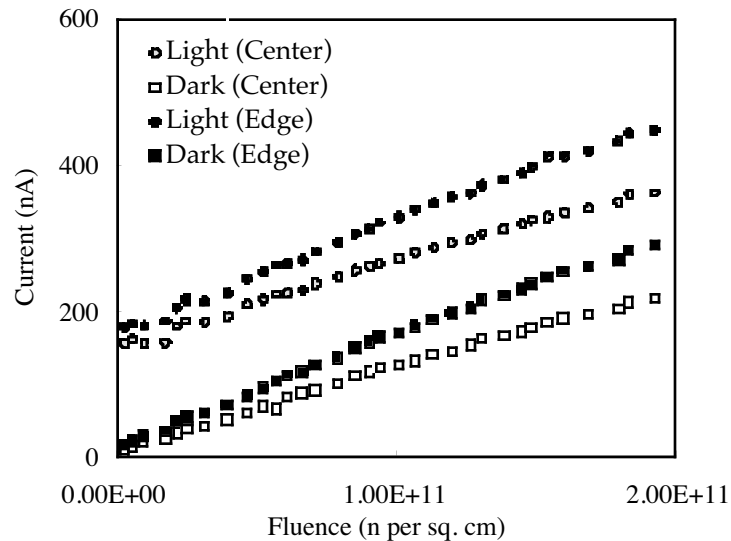


Fig. 8.12: Light and dark currents measured in 7-channel DEP HPD as a function of neutron dosage.

8.3.4 Magnetic field studies

During the 1996 CERN test beam, the 7-channel DEP HPDs read out the prototype HCAL while in the 3 tesla field of the H2 magnet. The response to muons improved consistent with a combination of scintillator brightening and focusing (the tube used in the 1996 run had a glass window and therefore some crosstalk at zero field). No reduction of gain or performance was measured, nor was mechanical stress a problem during cycling of the magnet current.

Both a 7-channel tube and a 25 channel tube were placed in the bore of a 5 tesla NMR magnet and their response to a light pulse (piped through a 1mm diameter fibre) was measured as a function of angle, accelerating voltage and bias. Since the B-field is so large, the

8. PHOTODETECTORS

photoelectrons rapidly gain energy and approach the regime where magnetic forces dominate over electric forces. The velocity $u=(1/B^2)E \times cB$ applies and the electrons follow the B field direction, making tight helical orbits with very small radii of curvature around the field axis. When the axis of the tube is at an angle q_B to the B-field, the motion of the photoelectrons corresponds to a sideways shift of $Dy \tan q_B$ superposed on their acceleration to the target, where Dy is the gap between photocathode and target. The cross field drift is only ~ 50 nm at this point. As the angle is increased, the signal in the centre pixel diminishes as the centroid moves off-centre. By offsetting the input light to re-establish the maximum, and plotting offset versus q_B , one can deduce the accelerating gap from the slope of the resulting straight line (Fig. 8.13). The fitted slope of $Dy=5.3$ mm is consistent with the vendor's value of 5 mm. At zero degrees, the gain in the tube with a glass window actually increased with magnetic field, due to focusing effects. The smallest accelerating gap consistent with safe application of a 15 kV accelerating voltage is 2 mm. Assuming this gap, and requiring a positioning of the HPD tube axis to within 5° of the B-field axis, the fibre bundles should be 400 nm apart to eliminate any crosstalk and gain shifts due to the B-field. Note that the dead region between pixels shown in Fig. 8.4 serves this purpose.

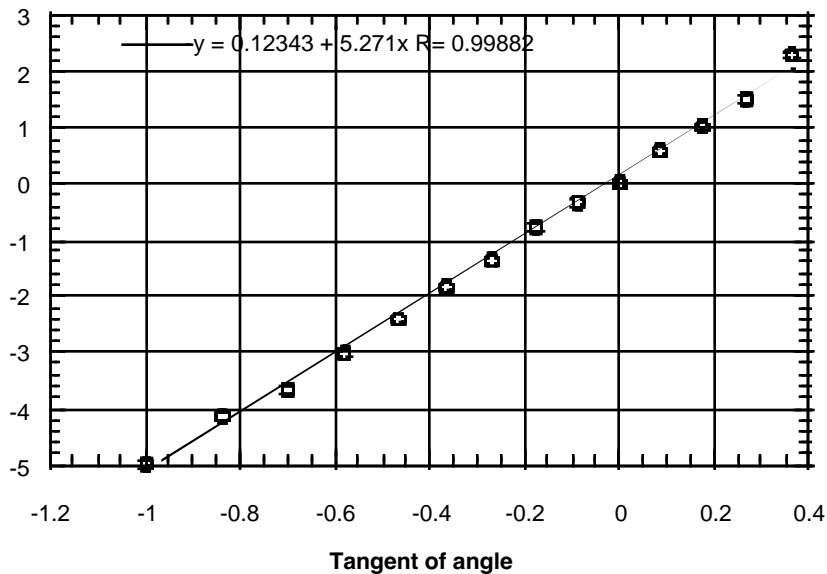


Fig. 8.13: Offset vs. $\tan q_B$ for a 7-channel DEP HPD in a 4.5 tesla field.

8.3.5 Crosstalk and uniformity

Since the target cost is \$100/channel, multi-pixel devices look promising. Crosstalk and uniformity were therefore measured in the lab for several different pixel configurations. Boundary scans such as Fig. 8.14 show that there is no dead space between pixels and that pixel to pixel uniformity is 2% or better. This high uniformity, coupled with the reproducibility of tubes with identical gain, means that there is no need for gain balancing either in the HV or in the readout electronics. Since the current required is very low, the HV distribution system can service multiple tubes with no problem. Optical crosstalk between pixels (with fibre optic window) will be less than 1% for the fibre bundle configurations and dead spaces between pixels planned for CMS. Capacitive crosstalk has been bench tested to be less than 2%. It can be reduced even further, by a thin aluminised layer and a drain structure between pixels. These improvements are being made in the new set of CMS diodes.

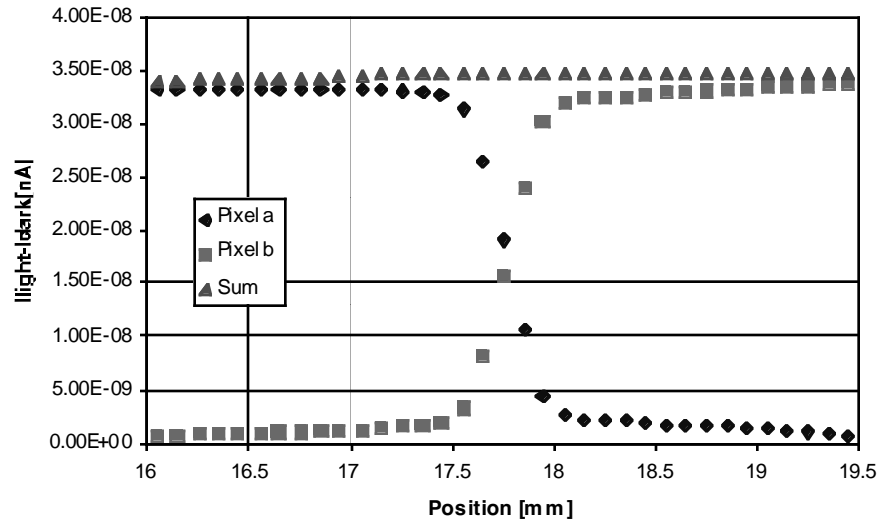


Fig. 8.14: Scan across pixel boundary of 25-pixel DEP tube using green light focused to a 250 micron diameter spot.

8.4 HPD DESIGN AND SPECIFICATIONS FOR CMS

Once HPDs were selected as the readout technology, specifications were drawn up and delivered to potential vendors. The specifications are listed in Table 8.2.

Since the longitudinal segmentation of HB and HE is so asymmetric, two different multipixel tube configurations are envisioned, one with fewer pixels which can accommodate bundles of up to 18 fibres and another with four times as many pixels, each of which services only up to 4 fibres per bundle. The latter will also be used for HB1/HE1 and HOB/HOE channels. In order to keep the total photodetector cost low, the ceramic carrier design will be the same for both types of tubes, as will the tube envelope. The proposed design for the two tubes is presented in Fig. 8.15. They are both on 25 mm diameter format. Each HCAL wedge consists of 4 j-partitions and 2 depth-partitions, each with 16 h towers. Since each photodetector box is associated with a wedge it contains four 16-channel devices for the HB-2 section and one 64-channel device for all the HB1 channels.

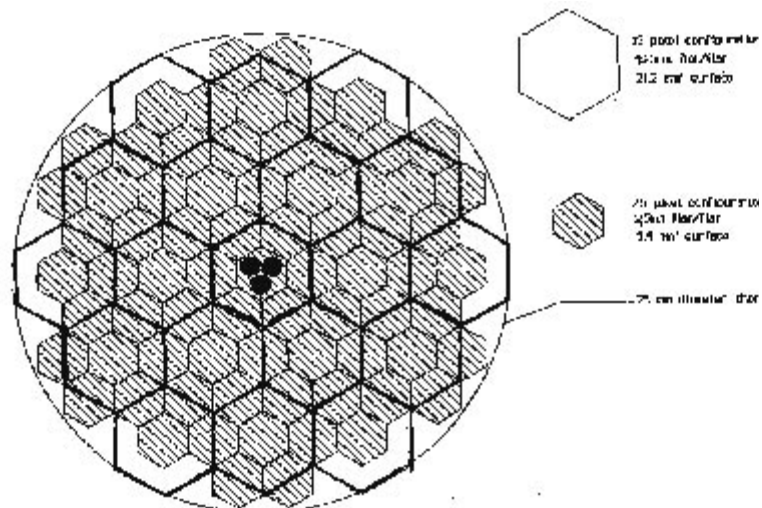


Fig. 8.15: Pixel configuration and tube outline of HPDs for CMS HCAL.

8. PHOTODETECTORS

Table 8. 2
CMS HCAL Photodetector Specifications

1. Photocathode:	Fibre optic window with S20 photocathode	
	Quantum efficiency:	>12% at 520 nm
	Radiant sensitivity:	>50 mA/W at 520 nm
	Dark counts:	<250 cnts/s/cm**2
	Photocathode uniformity:	better than 8%
2. Diode	Reverse current:	<20 nA at all bia voltages
	Pixel capacitance:	4 pF
	Channel and lead capacitance:	<25 pF
	Thickness uniformity	5 microns
	Inter-pixel resistance:	<100 ohms
	Junctions:	solder bump-bonding
3.Overall Tube Performance		
3.1 Gain	Operating gain:	>2000 electrons per photoelectron
	Gain variation channel/tube:	<2%
	Gain variation tube/tube:	<5%
	Min signal (muon)	10 photoelectrons (1 GeV equiv.)
	Max. signal (500 GeV hadron)	5000 photoelectrons
3.2 Linearity	Linear to 2% over this range:	(1 pe - 5000 pe or 12 bits)
3.3 Noise	Noise floor:	2000 rms electrons equivalent to 1 pe response
3.4 Crosstalk	Optical crosstalk:	<1%
	Capacitive crosstalk	<2%
3.5 Timing	Rate dependent gain shift:	<1% in all pixels
	Step input : rise time	<8 ns
	fall time	<8 ns
	Transit time spread	<1 ns
3.6 Magnetic Field	Resistant to magnetic field to	4 tesla
	Crosstalk	<2% at 5 degrees off-axis (0-4T)
	Gain reduction	<5% at 5 degrees off-axis (0-4T)
	Implications:	accelerating gap < 3mm used pixel perimeter plus interpixel gap > 400 microns
3.7 Pixel Size	Two types of tube required: Pixel size (with B-field allowances a specified by 8.3) must allow for bundles of:	a) 19 0.94-mm-diam plus thin calib fibres b) 3 0.94-mm-diam plus thin calib fibres plus B-field allowance as specified by 3.6.
3.8 Lifetime	After integrated radiation dose of 10 ¹¹ n/cm2 and 15C of integrated charge.	leakage current < 100nA fluctuation in - PC response <5% - dark counts <5% - uniformity remains

		as specified in 1. And 3.1
3.9 Pixel Failure	Number of pixel out of specifications:	zero
	Number of pixels failing over 10 years due to leakage current: due to internal flaws:	1 or less 2 or less
Cost Schedule	Final cost needs to average to under \$100/channel	\$100/channel

8.5 QUALITY CONTROL AND INSTALLATION

Quality control stations will be established at several locations. Three parallel processes will occur simultaneously. A few tubes will be left in the lifetime testing station for accelerated lifetime testing under various conditions. The rest will move through two other stations, one of which will concentrate on gain, rate dependence, signal-to-noise, and capacitive crosstalk in pulsed mode with the appropriate preamp connected. The second station will do DC scans of the photocathode and diode to determine uniformity and crosstalk. It will also do a trending histogram of the leakage current from all pixels for both long-term stability and short term rms fluctuations relevant to the source measurement. All phototubes go through both test stations.

8.6 HF PHOTODIODE SPECIFICATION

The HF photomultiplier specification is based on test beam performance of prototypes which used common low cost PMTs. During the test beams in 1994-6 with 3 different prototype modules, standard 5 cm (2") bialkali glass window PMTs (Hamamatsu R329[1], Philips XP2020, Philips XP2020Q) were used with no difficulty despite the low signal levels from the quartz fibre calorimeters. Fig. ADC distributions for high energy hadrons showed no tails from radiation punch-through induced pulses in the large PMTs, which were placed behind and 10 cm radially away from the edge of the back of the calorimeter, oriented with their axis perpendicular to the beam axis.

The specifications for the PMT, therefore, follow closely the specifications of the tubes used in the prototype work, with the some added requirements for operation in the LHC environment and the HF design.

In general, the selected tubes will be smaller than the PMTs used in the test beam to match the size of the fibre bundles and minimise the projected area of the PMTs to background radiation. Lower gain, will be utilised as well to match the low input noise afforded by the readout electronics and to increase the lifetime of the PMT (total charge drawn from the anode). However, in the main, the PMT are similar to most calorimeter PMT used in existing experiments. The basic HF phototube properties are determined by requirements of:

- a) dynamic range;
- b) area of fibre bundles;
- c) average and peak currents;
- d) tube lifetime;
- f) counting rates;
- g) gain sufficient for 1 p.e. as a least count separated from pedestal in the readout;

8. PHOTODETECTORS

h) operation of HF in a hundred Gauss of magnetic field at most.

The latter requirement allows standard low cost focused dynode PMT when sufficiently shielded with iron cylinders and metal. The high neutron flux at the location of the HF PMTs places a requirement that they are radiation resistant. For this reason we chose quartz (synthetic silica) window PMTs.

The maximum dynamic range of 1 p.e.- 1,500 p.e is modest, corresponding to ~ 2 GeV - 3 TeV for jet energies in one tower, a very unlikely occurrence but possible. Thus, the linear dynamic range required in HF is for the PMT is no more than $\sim 3,000$ and should present no difficulty for most dynode-gain technologies.

An $h=5$ tower may be exposed to as much as 100 GeV/crossing at 40 MHz, requiring a long-lived PMT (~ 30 -40 C/year of operation at a gain of 10,000), generally achieved by operation at lower PMT gains followed by very low noise electronics. The gain requirement depends on the noise level of the electronics. If the noise level is $\sim 10,000$ electrons for the readout at the end of a 2 m cable connecting the PMT to the readout electronics, a gain of $> 8 \times 10^4$ is sufficient for a S/N of 8 at the 1 p.e. level essential for the low energy response of the HF. The S/N level of ~ 8 is chosen so that 1/4 p.e. level can be discriminated and counted at least a 1:1 S/N level, and so that there is an additional factor of 2 in gain possible if the gain sags during the experimental conditions or if additional gain is needed for cable driving and to overcome additional electronic noise. The 1/4 p.e. discrimination is necessary to:

- a) determine accurately the shape of the 1 p.e. ADC spectrum which corresponds to $\sim 1(2)$ GeV electromagnetic (hadronic)energy;
- b) to have some additional safety margin in case of a loss of PMT gain during operations or in case of unanticipated electronic noise (widening the pedestal to a few channels for example), and
- c) to enable both ~ 1 MeV source calibration photons and possibly muon signals to be recorded in the test beam and off-line. Note that ~ 1 MeV source calibration photon can generate on average at most a 1 p.e. pulse when a Compton electron fully crosses a fibre at 42° . A higher noise level in the electronics will necessitate a higher gain PMT.

The very short optical pulse from the Cherenkov light, co-temporal with the relativistic part of the shower, and only 7-8 ns wide pushes up peak current linearity requirements, but the low light levels keep peak currents at modest levels, < 25 mA, easily realised by commercial PMT. If the fibres were bundled as $D_h \times D_f$ physics towers, the largest fibre bundles (low h) are matched by PMT with photocathode diameters of about 20 mm. If the fibres are bundled together from the fibres collected from 10 cm \cdot 10 cm and 5 cm \cdot 5 cm bricks, the tube diameters with areas equal to the fibre bundle diameter are 14 (7) mm respectively. It is of some advantage to standardise on the maximum or larger PMT diameter. Since the higher h tower PMTs receive more light by nearly an order of magnitude over the $h = 3$ towers and require a higher level of charge drawn per unit area of anode, it is reasonable to select a PMT in the diameter range of 15-20 mm for the photocathode for all towers, reducing complexity and lowering cost due by economies of scale.

After- and pre-pulsing at typical levels from commercial PMT will not be a problem for this experiment, and will be less than the noise pulses at the few p.e. level from ambient radiation (neutron, photon), inducing on average 0.5 p.e. noise per tower on each gating.

The risetime requirement derives mainly from the desire to reserve the potential to separate beam-gas and interactions in the quadrupoles from genuine beam-beam events by timing, but long enough so that peak currents are not a problem for the PMT. Rule-of-thumb dictates timing

at $\sim 20\%$ of the risetime is reasonable. Combining requirements gives a risetime < 2.5 ns, and > 1 ns.

An important requirement is that the transit time through the PMT be less than the bunch interval time, in order to minimise hysteresis effects in the PMT. We have demonstrated (Fig. 8.16) that a PMT with a transit time of 8.5 ns (Hamamatsu R5900) can easily reproduce a 40 MHz optical pulse train generated by a blue LED, at a level of ~ 30 p.e. (about 60 GeV jet energy in HF) at a gain of $\sim 1 \times 10^5$. This is thus an important requirement, and the baseline PMT chosen has a maximum transit time specification of 16 ns.

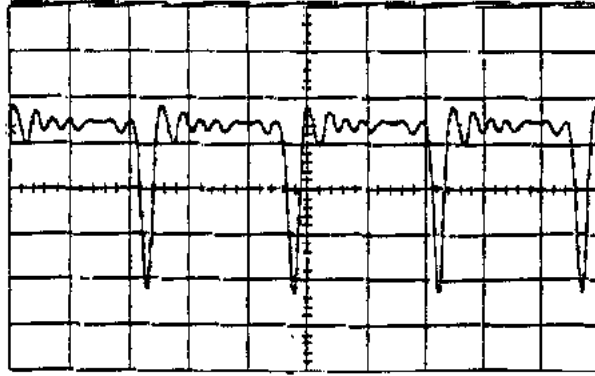


Fig. 8.16: 40 MHz optical pulse train using an R5900 (20 mV/div x 10ns/div).

The PMT lifetime requirements are derived from the rates induced at high h by the beam. At $|h| > 5$, we anticipate that a PMT at a gain of 10,000 will deposit ~ 32 C/year on the anode. The anode lifetimes are typically ~ 350 C. We have demonstrated pulsed current lifetimes of the miniature PMT in excess of > 300 C. Fig. 8.17 shows such a lifetime test.

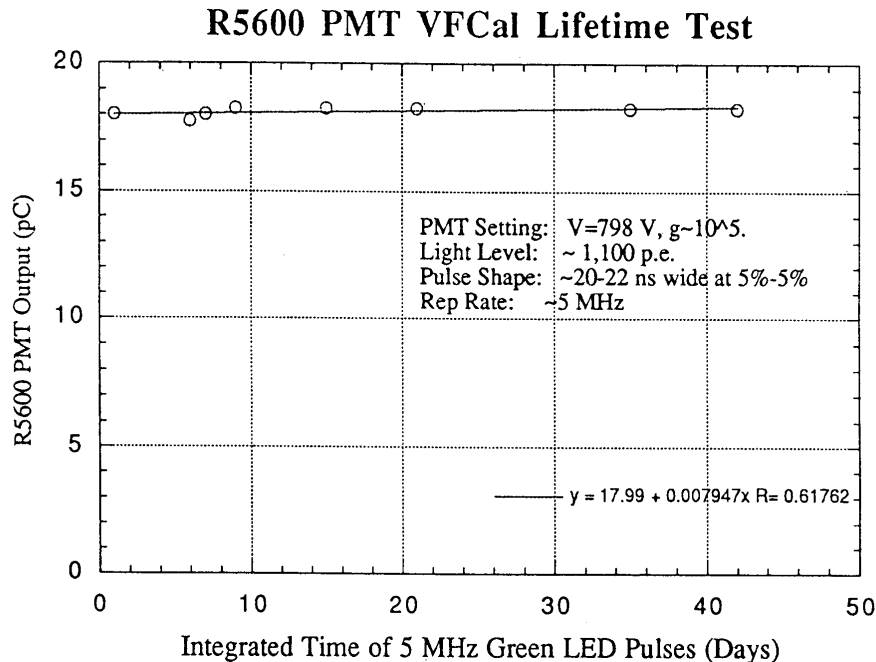


Fig. 8.17: PMT lifetime test at 1,100 p.e./pulse (~ 2 TeV/pulse) at 5 MHz.

8. PHOTODETECTORS

Thus the PMTs on the towers of highest pseudorapidity, accounting for ~104 PMTs, may have to be changed on an annual basis, if the design specification for the QIE noise is greatly exceeded. Alternatively, one could accept a S/N level of 1 in the highest η towers. Lowering the gain to ~10,000 (i.e. by a factor of 10) would increase the lifetime to 10 years.

Table 8. 3
HF PMT Specifications.

Diameter:	$f_{\text{cathode}} > 13 \text{ mm}$
Q.E.	$\pm 15\%$ 400-500 nm; $\pm 25\%$ @ 400 nm
Cathode Uniformity	$< -10\%$, -2 mm point, within 0.9 dia.
Photocathode lifetime:	$> 10 \text{ mC}$ drawn from cathode, with $g > 0.9g_{\text{initial}}$
Gain:	$> 5 \times 10^4$ per 10,000 e- noise
Single p.e. Resolution	rms/mean of single p.e. peak $< 50\%$
Linearity, Pulse	-2% from 1-3,000 p.e.
Peak Current	$I_p \pm 25 \text{ mA}$ -2% (per 2 ns t_{rise})
t_{transit}	$< 25 \text{ ns}$
t_{rise}	$\pm 2.5 \text{ ns}$ (10%-90%)
Pulse Width t_{FWHM}	$\pm 8 \text{ ns}$
Gain (1/2) Lifetime:	$\pm 320 \text{ C/year}$ ($g=10^5$, 100 GeV per 25 ns)
Average Current:	$\pm 60 \text{ mA}$
Stability:	$< -3\%$ 24 hours; $< 2\%$ short term
Tube-Tube Uniformity:	Gain*QE within -1% by HV adjustment
Window	Quartz, thickness: $< 2 \text{ mm}$
Window Coatings	Transmission: $> 90\%$ 400-600 nm, $< 10\%$ 300 nm He Permeability: \pm borosilicate glass
Envelope	Opaque & Conductive coating
Radiation Dose	10 kRad/year: $< 90\%$ QE*G loss $3 \times 10^{12} \text{ n/cm}^2 \text{ /year}$: $< 50\%$ QE*G loss

Basic PMT requirements derived from the above considerations are summarised in Table 8.3. Note that the PMT requirements include:

- Reduced Radiation-Induced Pulses: Where possible, compact vacuum envelope, compact dynodes, opaque envelope, and thin photocathode window PMT will be selected, in order to minimise the amount of false pulses from neutrons, gammas and muons crossing the PMT itself. Additionally, materials in the PMT should be chosen to minimise neutron activation and fast neutron reactions. Alternative glasses (especially fused quartz) to boron-containing ones are preferred.

These background pulses associated with the particles incident on the calorimeter are not anticipated to be large in any case. Test beam data show that the background pulses induced on

an XP2020 5 cm diameter PMT placed directly behind the calorimeter prototype have an average value of ~ 1.3 GeV with an rms of ~ 1 GeV with 350 GeV pions incident. Note that the ADC gate was 60 ns during this testing. Similarly, a miniature R5600 (8 mm cathode) had negligible induced pulses when similarly placed behind the prototype calorimeter in the test beam.

The radiation background calculations indicate that about $2.7 \cdot 10^{-5}$ mip/cm²/crossing will be at the front face of the PMT, or about $5 \cdot 10^{-5}$ per PMT per crossing. A study of background induced in PMT by mips and photons through the front window of PMT was carried out by the ITEP group in HF[2]. Fig. 8.18 shows the probability as a function of $N_{p.e.}$ to obtain $N_{p.e.}$ for mips passing through a 1mm thick PMT window (R5600). The mean response to a mip is 6.06–3.58 p.e. This would correspond to a noise of 1.2 p.e./crossing, or about 2.5 GeV/crossing in noise from mips. Note that this noise floor may soften the gain requirements on the PMT.

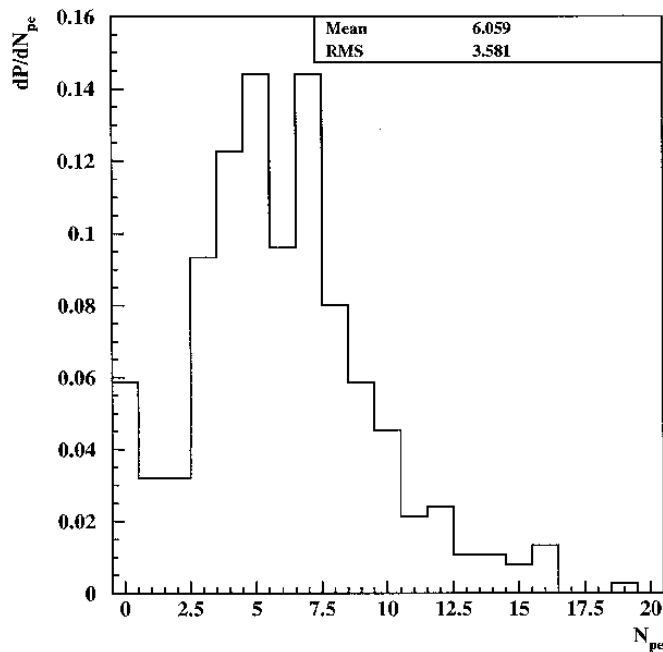


Fig. 8.18: The probability as a function of $N_{p.e.}$ to obtain $N_{p.e.}$ for mips passing through a 1mm thick PMT window (R5600)[2].

The probability for a ~ 1 MeV (^{60}Co) photons to induce pulses in an 8 mm diameter, 1mm thick window PMT (R5600)[2] has a mean is 0.25 p.e./photon, and the efficiency (probability of 1 p.e. or greater) for counting a photon is 15%. The radiation dose calculations indicate that there will be $\sim 10^{-4}$ photons per PMT/crossing impinging on the PMT windows, or a noise floor, of 0.33 p.e. per crossing from photons.

- b) Helium Partial Pressure: Envelope and coatings to reduce the permeability to He are essential. The photocathode window may be overcoated with a thin low index silicone polymer, both for antireflection coating and for He permeability resistance, if it can be proven for radiation damage. This may be demanded by He partial pressures anticipated in the hall. Alternatively, a CVD coating of MgF or CaF may be specified in the PMT bid. Permeability to He in quartz is 1-2 orders of magnitude larger than in glass. The PMT housing and gas system will reduce ambient He pressure by more than 10^{-3} .
- c) Removable of UV component: Because the UV light generated in the quartz fibres is subject to degradation by radiation damage, the UV light is cut-off by a filter system. This system

8. PHOTODETECTORS

will either use a Schott glass filter of 1 mm thickness[2], or dielectric coatings with short wavelength cut-offs. These may include an ITO (indium tin oxide) conductive coating at the HV of the photocathode which will protect the cathode also from electrostatic effects when connected to the cathode voltage.

The ITO coating and the antireflection coatings are resistant to He diffusion. Thin-film coatings are generally known to be radiation hard[3,4] because (a) a coating thickness $< \sim 1\text{-}2$ nm requires an enormous dose to create a large optical density on such a thin film, (b) it is difficult to change the electron density and hence the index n by radiation, and (c) dielectric coatings with high resistivity on the order of 1 wavelength have low absorption. The magnesium fluoride and/or silicon monoxide films likely to be selected for the HF PMT.

The PMT requirements outlined above are met with a 19 mm (15 mm cathode OD) PMT from Philips and Hamamatsu, and by the 25 mm (21 mm OD cathode) R5800Q. The desired baseline PMT is a 10 stage, in-line dynode Hamamatsu PMT, the R4125, with a typical (maximum) gain of about 10^5 (10^6), developed for high linearity. This tube is available with a special coating to make the walls black and impermeable, and with a quartz window only 2 mm thick[5].

In test beams, the very lowest background PMT is the metal envelope, metal-mesh dynode PMTs from Hamamatsu [Table 8. 4], the R5600, with an 8 mm diameter photocathode, and the R5900 (18 mm square cathode). The diameter of the R5600 is matched to the size of the bundles from the highest h towers. The window material may be made as thin a 0.8 mm, greatly reducing Cherenkov light. Additionally, the metal channel mesh dynode stack is only 6 mm thick for 8 stages of gain (up to 10^5), which reduces the cross-section for induced pulses from radiation backgrounds. The metal mesh family of Hamamatsu PMT are also preferred because of the short transit times (< 9 ns).

Table 8. 4
Photomultiplier tube summary.

	R4125	XP1918	R5800	R5600
Diameter	15 mm	15 mm	21 mm	8 mm
Gains	10^5 /1,100 V	10^5 /900 V	10^5 /800 V	10^5 /900 V
Q.E.:	27% /400 nm	26% /400 nm	27%/400nm	27%/400n
t_{rise} :	2.5 ns	2.4 ns	1.5 ns	0.7 ns
t_{transit} :	16 ns	23 ns	21 ns	< 8 ns
Pulse Linearity	-2% 100 mA	-2% 80 mA	-2% 100mA	-5%,30 mA
I_{ave} :	100 mA	200 mA	100 mA	100 mA

Refinements in the choice of baseline PMT may be made at the time of order, depending on development efforts by commercial manufacturers. There are clearly a number of reliable alternatives, and performance is not a serious issue. It is likely in order to decrease the transit time further, and to increase the linearity and lifetime, we may specify PMT variants of the R4125 or XP1918 with 8 stages rather than 10 stages. The transit time should decrease to ~ 13 -

14 ns in the R4125. At present, the best compromise between price and performance is the R4125/XP1918 types, while the best price is the R5800Q.

8.7 RADIATION DAMAGE

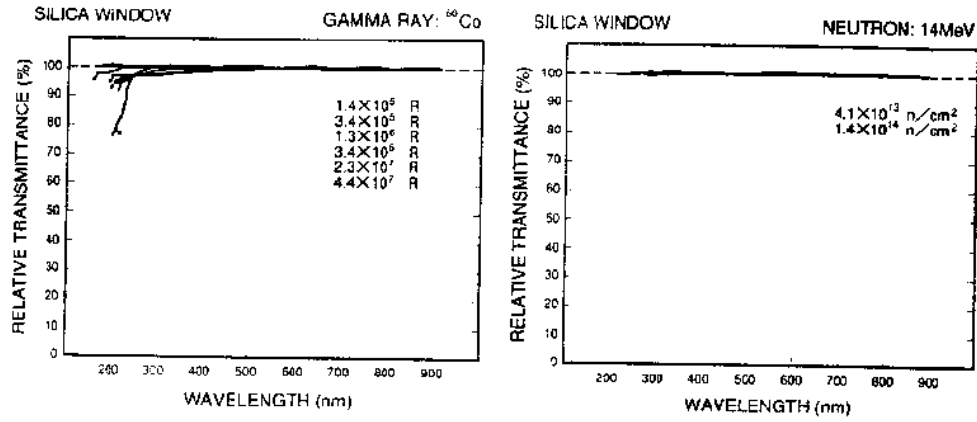
The HF PMTs are sufficiently shielded by the HF itself, the HF shielding, and by the bulk of CMS that radiation damage will be minimal. The HF PMT are located at over 1 m in radius, from the beam pipe and over 14 m from the IP, and are enclosed in a robust shield to absorb neutrons. Radiation calculations indicate that the HF PMT should receive a radiation dose of about 1 krad/year, with about 10^{10} n/cm²/year.

The dynodes are intrinsically radiation hard[6]. A study of the dynode radiation hardness up to 10 Mrad of ⁶⁰Co indicates no change to the dynode gain (ibid.). The photocathode materials, a bialkali photocathode (NaK₂Sb or Cs₂K Sb), is classed as a very loosely bound amorphous semiconductor; *i.e.* a simple stoichiometric ratio of materials made by alkali diffusion into a thin amorphous Sb at temperatures well-below that needed to form crystalline materials. This structure is not affected strongly by dislocation defects from radiation bombardment. The principle cause for radiation damage failure is the darkening of glass envelope windows, activation of the window material producing phosphorescence (thermal luminescence), and insulation failure. Fig. 8.19 shows the radiation-hardness of 3 major types of glass used in PMT, from the Hamamatsu handbook, for photons (left) from 144 krad- 44 Mrad, and neutrons (right) from $\sim 4 \times 10^{13}$ - 2.5×10^{14} n/cm²[7].

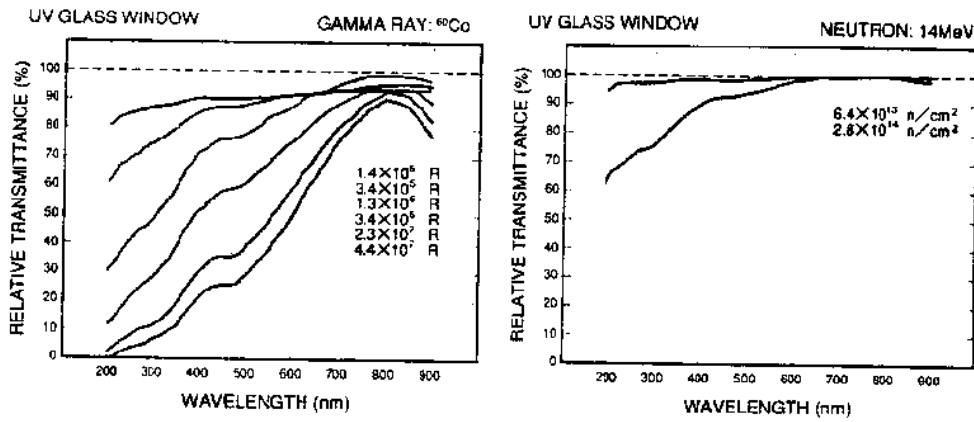
Additionally, induced fluorescence, phosphorescence and “scintillation” occurs with radiation on standard glass photocathode substrates. Fig. 8.20 from the Hamamatsu PMT Handbook shows the increase in dark current with a very low dose of radiation (10.5 rad) in borosilicate glass[8].

The PMT candidates are undergoing tests in Hungary to determine the extent and properties of radiation damage. They operate at up to 10^{14} n/cm² with little effect on gain. However, PMT radiation damage occurs first in the glass window. The glass of the envelope may turn black, with little effect on the PMT gain operation. We have observed low levels of induced phosphorescence in the window using UV-glass from Hamamatsu. We anticipate that the high purity synthetic quartz version will not have this effect. Other quartz window PMTs have been shown to operate at levels of exposure up to 50-100 Mrad of ⁶⁰Co radiation. For example, EMR Photoelectric, Princeton, NJ, has demonstrated operation of quartz window PMT up to 100 Mrad (type 730N-01-13, 1” end-on PMT) for operation in the cosmic ray environment of space which uses a thinned silica glass window and a standard bialkali photocathode[9]. Additionally, some PMT may use insulator materials which are not fully radiation-hard for the connector pins or for dynode stand-offs. Alumina- and lead-oxide-based ceramic dynode stand-offs are specified, and used in the PMT selected.

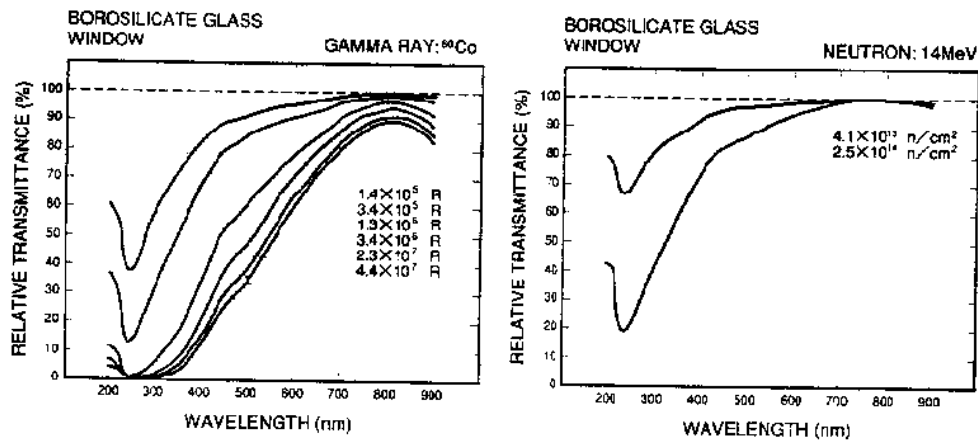
8. PHOTODETECTORS



Transmittance variations of a synthetic silica window when irradiated by gamma rays and neutrons



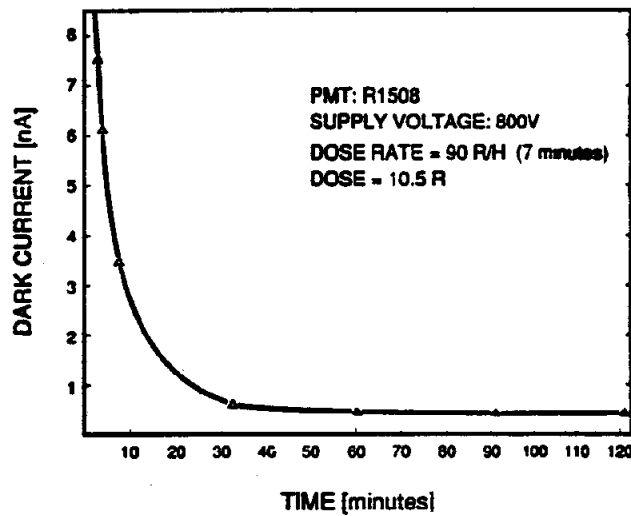
Transmittance variations of a UV glass window when irradiated by gamma rays and neutrons



Transmittance variations of a borosilicate glass window when irradiated by gamma rays and neutrons

Fig. 8.19 : The radiation-hardness of 3 major types of glass used in PMT, from the Hamamatsu handbook, for gammas (left) from 144 KRad- 44 MRad, and neutrons (right) from $\sim 4 \times 10^{13}$ - 2.5×10^{14} n/cm².

GLASS SCINTILLATION



Dark Current Variation After γ -Irradiation (Borosilicate)
Hamamatsu PMT Handbook (1994)

Fig. 8.20: The increase in dark current with a very low dose of radiation in borosilicate glass.

8.8 QUALITY ASSURANCE

The PMT quality for HF will be assured by a test cycle that occurs in 3 forms: at the manufacturer, testing and preselection as they arrive, and beam and calibration tests during the installation period. The purpose of these specifications and tests is to assure that a PMT can be replaced with the confidence that any PMT will function within 2% of any other PMT, with control of the HV alone. Spare PMT will be ordered (10%) to allow for preselection matching, breakage, and failure.

For the manufacturer, a detailed set of specifications, similar to the ones shown above, will be proposed in the bidding process, but with an appropriate negotiation so as not to increase the price inordinately due to very extensive manufacturer testing or pre-selection. Because of the low light levels of the HF signal, the quantum efficiency and cathode uniformity are key issues in the specification. At present, the industrial capability is available to guarantee a point-point uniformity over 2mm x 2mm areas of -5% out the edge of the usable photocathode. This uniformity is sufficient, because the light from each fibre will be pseudorandomized by a light mixer in such a fashion that each fibre will illuminate more than 50 % of the photocathode area.

The PMT will be delivered half each to 2 identical test stations for testing, with duplicate measurements for comparison made on 10% of the PMT. These stations will utilise pulsed light systems (laser and LED), radiSOURCE-scintillator constant light sources, and data acquisition to measure: (a) gain vs HV, (b) pulse shape, (c) single photoelectron level, (d) PMT noise at the 1/4 p.e. level, (e) the linearity of the response from 1-2,000 p.e., (f) relative gain changes at 0.1, 1, and 40 MHz. A fibre scanner will quantify photocathode non-uniformities on a 5 mm scale. The quantum efficiency at several wavelength pass-bands (in a range from 300-600 nm) will be measured with temperature controlled scintillators + alpha source (NaI, BGO, CaF₂ and BaF₂) with optical filters, which serve as constant light sources.

8. PHOTODETECTORS

The PMT can be delivered at a rate of about 200/month, requiring a 6 month lead time to start delivery, 17 months for the PMT fully delivered order, or 2 years to complete the PMT acquisition and testing. We budget a total of 1 hour each to unpack, test, label, repack, and enter, merge publish & archive data for ~4000 PMT. The selection database will be maintained for each PMT together with the base and front end electronics.

References

- [1] Hamamatsu Photonics Corp. Bridgewater NJ.
- [2] V. Gavrilov et al., Sensitivity of Photomultipliers to Protons and Gammas, CMS TN/95-146 (15 Nov., 1995).
- [3] Schott Glass Inc.
- [4] A. Holmes-Sidle and L.Adams, Handbook of Radiation Effects, (1994) Oxford U.P., Oxford, UK.
- [5] J. Wong and C.A.Angell, Glass: structure by spectroscopy (1976) Dekker, Basel.
- [6] S.Belianchenko et al., Study of PMT Radiation Hardness, IHEP 96-90 (1996) (submitted NIM).
- [7] Photomultiplier Handbook, Hamamatsu Corp., 176 (1994).
- [8] Photomultiplier Handbook, Hamamatsu Corp., 177 (1994).
- [9] M.M.Birnbaum, R.L.Bunker (JPL, Pasadena, CA), J.Roderick, and K.Stephenson (EMR Photoelectric, Princeton NJ), "Development of a Radiation-Hard Photomultiplier Tube" (1984) EMR Photoelectric Publication, Princeton, NJ, and published in the American Institute of Aeronautics and Astronautics (AAIA) Guidance and Control Symposium Proceedings, AIAA-84-1852, (Aug. 20-22, 1984).

TABLE OF CONTENTS

8.1 HADRON CALORIMETER PHOTODETECTORS312

8.1.1 HB/HE REQUIREMENTS312

8.1.2 HOB AND HOE PHOTODETECTOR REQUIREMENTS313

8.3 HPD CHARACTERISTICS FROM TEST BEAM AND RADIATION EXPOSURE ...317

8.3.1 RESPONSE TO PARTICLES - MUONS317

8.3.2 DC RESPONSE AND CALIBRATION TO Cs SOURCE318

8.3.3 LIFETIME AND RADIATION DAMAGE318

8.3.4 MAGNETIC FIELD STUDIES319

8.3.5 CROSSTALK AND UNIFORMITY320

8.4 HPD DESIGN AND SPECIFICATIONS FOR CMS321

8.5 QUALITY CONTROL AND INSTALLATION323

8.6 HF PHOTSENSOR SPECIFICATION.....323

8.7 RADIATION DAMAGE.....328

8.8 QUALITY ASSURANCE331